

## PHYSICAL AND NUMERICAL MODELING OF HARBORS AND SHORE PROTECTION MEASURES

### *Modélisation physique et numérique de mesures de protection portuaires et d'aménagement de plages*

Fadi, E., Hachem<sup>1</sup>, Azin, Amini, Jean-Louis, Boillat  
Laboratory of Hydraulic Constructions (LCH-EPFL), Ecole Polytechnique Fédérale de Lausanne,  
Station 18, 1015 Lausanne, Switzerland. Phone: +41 (21) 693 24 01, Fax: +41 (21) 693 22 64.  
[fadi.hachem@epfl.ch](mailto:fadi.hachem@epfl.ch), [azin.amini@epfl.ch](mailto:azin.amini@epfl.ch), [jean-louis.boillat@epfl.ch](mailto:jean-louis.boillat@epfl.ch)

#### KEY WORDS

Water wave mechanics, wave reflection and refraction, protection dikes, beach erosion, groins structure, shoreline stabilization, beach profile.

#### ABSTRACT

*The expansion project of the "Port de la Nautique" and the creation of adjacent new beaches on the "Lac Léman" in Geneva is currently under survey. In the conceptual and study phase, numerical- and physical-scaled models have been exploited at the Ecole Polytechnique Fédérale de Lausanne (EPFL). The objectives are to analyze the currentology and the wave's field inside the protected zone of the harbor and their influence on the stability of the new beaches. The numerical modeling is driven by two models at different scales. The large scale model provides the boundary conditions to the small one which is used to estimate the circulation of water in the new harbor and to predict the erosion and deposition processes inside the harbor and along the beaches. The physical model is built using distorted scale factors inside an experimental wave tank that covers the same area as the small numerical model. It aims to optimize the project and to confirm the numerical results concerning notably the wave heights inside the harbor and the sediment transportation processes all along the beaches. The results obtained by the complicity of the numerical and physical simulations helped to converge toward an optimal design locations, orientations, and types of the protective dikes of the port as well as the geometric configuration and number of groins and the choice of the suitable backfill grain size for the new beaches.*

#### RESUME

*Le projet d'agrandissement du Port de la Nautique et de création de plages adjacentes sur le lac Léman à Genève est actuellement à l'étude. Dans la phase conceptuelle et de dimensionnement, un modèle numérique et un modèle physique à échelle réduite, ont été exploités à l'Ecole Polytechnique Fédérale de Lausanne (EPFL). Ces modèles ont pour objectifs d'analyser la courantologie et les champs de vagues dans la zone protégée du port ainsi que leur influence sur la stabilité des plages. La modélisation numérique est conduite sur deux modèles emboîtés, à grande et à petite échelle. Le grand modèle fournit les conditions d'entrée au petit modèle dont le rôle est d'estimer la circulation de l'eau et d'évaluer les processus d'érosion et d'alluvionnement dans le port et sur les nouvelles plages. La modélisation physique est réalisée à échelle distordue dans un bassin à houle couvrant la même superficie que le petit modèle numérique. Le modèle physique a pour mission de confirmer les résultats numériques obtenus concernant notamment les hauteurs des vagues à l'intérieur du port et les processus de transport sédimentaire le long des plages. Il sert également à optimiser le projet. Les résultats obtenus par la complémentarité des modélisations numérique et physique ont permis de converger vers une solution d'aménagement optimale concernant les emplacements, orientations et types des digues de protection du port ainsi que la configuration des épis et le choix de la granulométrie sédimentaire des nouvelles plages.*

---

<sup>1</sup> Corresponding author

## 1. INTRODUCTION

The creation of a new public parc and beach and the expansion of the “Port de la Nautique” harbor in Geneva are actually under investigation. A plan view with the main element of the project, the actual and future coastline limits and the Rhône river are shown on Figures 1.a and 1.b. The water level of the lake fluctuates between 371.7 m.a.s.l. and 372.3 m.a.s.l. The water flowing outside the lake is controlled by the “Seujet” Dam and varies between 100 and 500 m<sup>3</sup>/s.

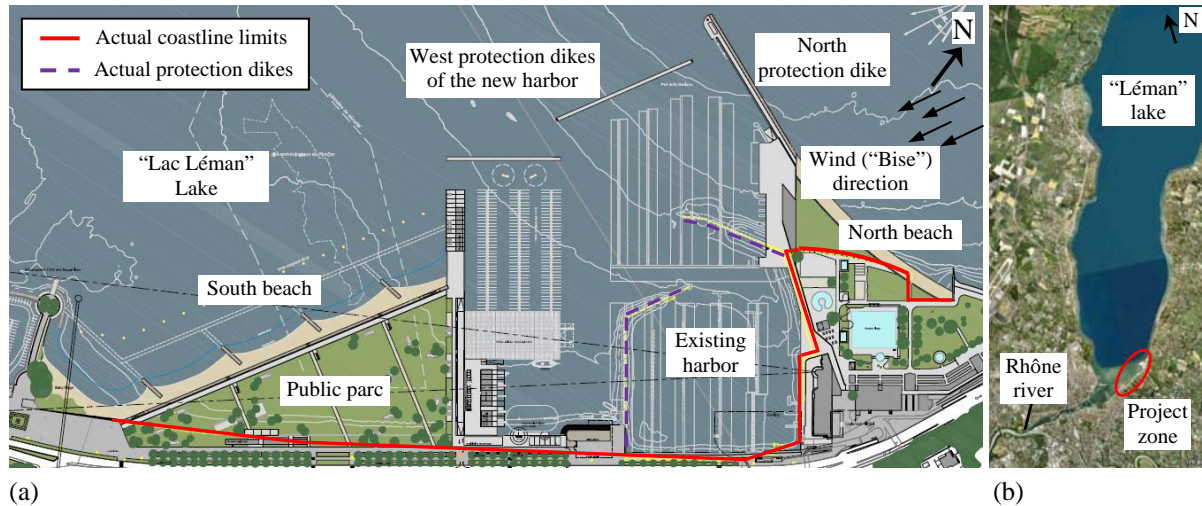


**Figure 1:** Plan view of the project. a) The actual and future harbor, north and south beaches, and the direction of the “Bise” wind, b) the layout of the south-west part of the lake with the Rhône river.

The meteorological analysis using data from the “Genève-Cointrin” station and from in-situ measurement campaign reveals the existence of two dominant wind directions in the project zone; the south-west and the north-east winds. The direction of the maximum fetch line of 30 km long relative to the project zone, is 30° from North. The shear forces created by the combination of the north-east wind, known as “Bise”, with the maximum fetch direction, generates the critical wave field for the project. The wind and wave parameters taken as input data for the numerical and physical modeling are depicted in Table 1. The return period, velocity, and blow duration of the wind is determined using the “Intensity-Duration-Frequency” curves established from the “Genève-Cointrin” station data between years 1979 and 2005. The significant height and period of waves in deep water are estimated according to the Jonswap method [1,7].

Wind return period, $T_W$ (year)	Wind velocity, $V$ (m/s)	Wind blow duration, $t$ (hour)	Significant wave height, $H_s$ (m)	Wave period, $T$ (sec)
1	10.0	5	0.88	4.2
20	14.3	4	1.27	4.7
100	16.8	4	1.49	5.0

**Table 1:** Wind and wave field characteristics used in the numerical and physical simulations.

## 2. NUMERICAL MODELING

### 2.1 Software description

The numerical simulation was conducted using MIKE 21 software package. The following modules have been used herein: i) The Hydrodynamic module (HD) which simulates the water level variations and flow response to a variety of forcing conditions in lakes and coastal areas, ii) The Spectral Wave module (SW) which simulates the growth, decay and transformation of wind induced waves and swell in offshore and coastal areas, iii) The Elliptic Mild Slope Wave module (EMS) which enables to study the wave dynamics in coastal areas, and iv) The Sand Transport module (ST) which calculates the sediment transport rates on a flexible mesh (unstructured grid).

## 2.2 Numerical model

The courantology was simulated on a large-scale model covering an area of  $4.2 \times 4.5 \text{ km}^2$  (Figure 2.a). The topography and the offshore lines were obtained from the digital elevation model MNT25 from SwissTopo. Additional topographic points and construction details were added by hand to the small-scale model that covers an area of  $0.9 \times 1.5 \text{ km}^2$ . The latter was used to determine the wave height field inside the new harbor. Figures 2.a and 2.b show respectively the plan view and the 3-D view of the large-scale model. The limits of the small-scale model are also shown.

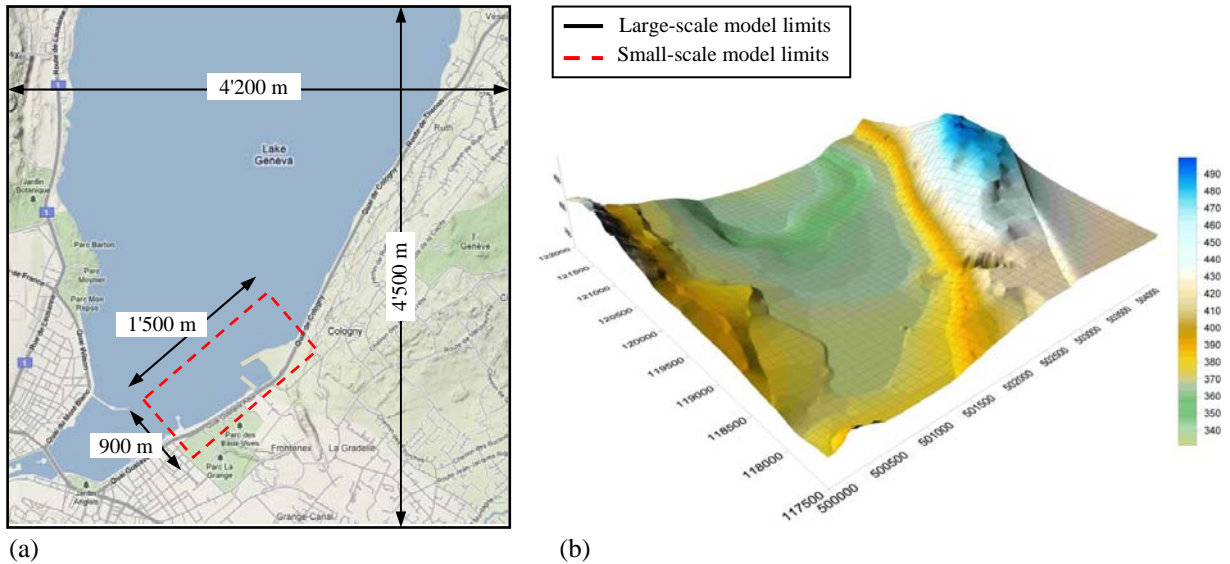


**Figure 2:** Large- and small-scale model limits for the numerical simulations. a) Plan view showing the areas covered by the two models, b) 3-D topographical view of the large-scale model.

## 2.3 Results and discussion

### 2.3.1 Courantology and water renewal duration

Different combinations including the two dominant wind directions with different characteristic discharge values of the extracted flow supplying the Rhône river have been simulated. Results show that the “Bise” effect combined with a low outflow rate generates a high velocity field of about 35 cm/s in the south beach foreshore. Therefore, a series of groins was required in this area to protect the beach sand from erosion. Under the same load combination, the future north dike reduces the current intensity near the north beach (Figure 3.b). The velocity field vectors inside the large-scale model is presented in Figure 3.a for a “Bise” return period of 1 year. Another zoomed plan view covering the project zone is shown on Figure 3.b. Inside the new harbor and under the south-west wind effect, a maximum circulation velocity of 9 cm/s was found.

Concerning the water renewal duration, results show that for  $100 \text{ m}^3/\text{s}$  in the Rhône river, the velocities inside the new harbor become very low. Among others, the construction of an open channel through the north dike was found to be an interesting solution to increase the circulation velocity up to 0.8 cm/s inside the future harbor. The water renewal duration near the north and south beaches was estimated around 6 to 8 hours.

### 2.3.2 Water waves

In purpose to estimate the intensity of erosion and deposition phenomena along the beaches, some processes affecting the wave propagation from deep into shallow water have to be considered. The most important propagation effects are refraction, shoaling and breaking of waves along the beaches. Inside the harbor, wave diffraction, transmission and reflection are the important phenomena to be investigated in order to design a safe and an efficient operational harbor.

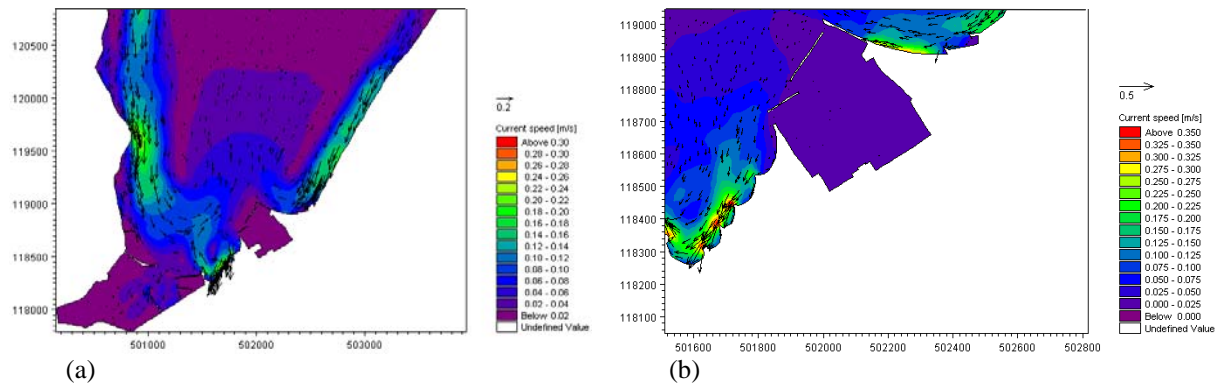


**Figure 3:** Current velocity field (m/s) under the “Bise” effect and for a flow of  $100 \text{ m}^3/\text{s}$  supplying the Rhône river. a) Entire large-scale model, b) Zoom on the project zone.

The above mentioned processes were simulated on the small-scale model using the results of the large-scale model as boundary conditions. For a “Bise” of  $T_W = 20$  years, Figure 4.a shows an instantaneous shot-view of the wave propagation field (crest and trough). The distribution of wave height inside the harbor is presented in Figure 4.b. In these simulations, absorption factors were allocated to the rockfill dikes and harbor’s walls. A complete reflective version, with concrete version of these structures was also analysed. The wave heights obtained in this latter case are shown for comparison on Figure 4.c. The four squares plotted inside the harbor represent areas in which the arithmetic mean value of the wave height was computed and compared to the corresponding measurements in the physical model.

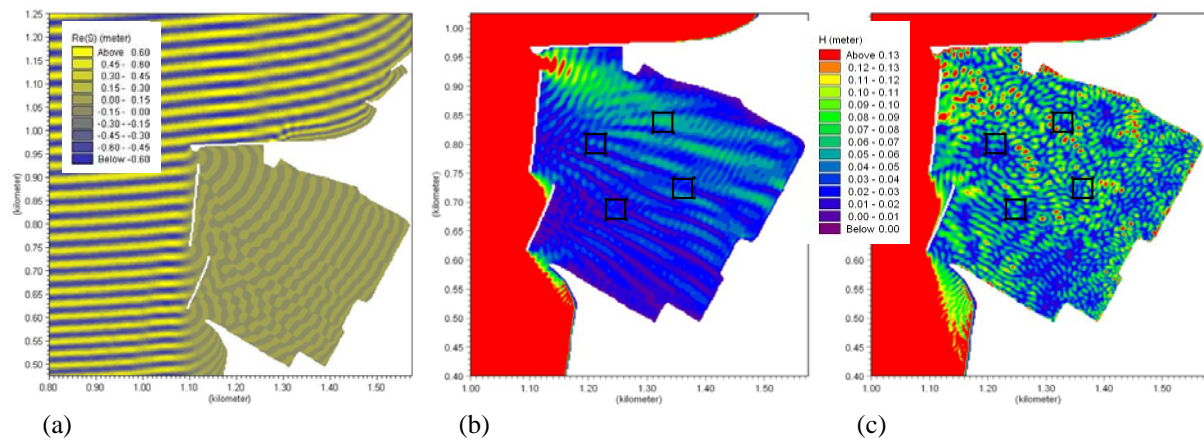


**Figure 4:** Numerical results of the wave propagation field for a “Bise” of  $T_W = 20$  years. a) Wave field (crest and trough) for absorbent harbor’s dikes and walls, b) Wave height inside the harbor for absorbent harbor’s dikes and walls, and c) Wave height inside the harbor for reflective harbor’s dikes and walls.

The numerical results reveal that with absorbent walls, the harbor is well protected except an exposed zone of about 50 m long located at the north-west side where the maximum wave height reaches 13 cm. In case of reflective walls, local zones with more than 13 cm of wave height are spreaded all over the entire area inside the harbor. The mean wave heights  $H_{mF}$ , calculated over the harbor area are presented in Table 2. The relative differences comparing  $H_{mF}$  to the mean wave height  $H_{mA}$ , simulated with the actual harbor configuration, are also given. It can be noticed that the consideration of absorbent walls and dikes leads to significant attenuation of the mean wave height inside the harbor. For the south wind waves, the future harbor is less protected than the actual one.

### 2.3.3 Sediment transport

The median sediment grain sizes ( $d_{50}$ ) considered in the simulations are 0.1 and 0.8 mm inside the harbor and along the beaches respectively. The results of the numerical simulation predicting the bed evolution after an equivalent prototype duration of 12 days and for a “Bise” of  $T_W = 5$  years are shown on Figure 5. Sections from A-A to D-D, drawn on these figures, were used to estimate the velocities  $U_{max}$  (m/s) of wave-induced water motion in the offshore zones.

Wind type	Harbor configuration	Walls and dikes	Mean wave height, $H_m$ (cm)	Relative difference (%)
“Bise” ( $T_W=20$ years)	Actual	Absorbent	4.4	
	Future	Absorbent	3.3	- 33.3
Reflective		9.8	+ 55.1	
South wind ( $T_W=100$ years)	Actual	Absorbent	7.1	
	Future	Absorbent	8.7	+ 18.4

**Table 2:** Mean wave heights over the entire harbor area in the actual and future harbor configurations under a “Bise” of  $T_W=20$  years and the south wind of  $T_W= 100$  years ( $H_s = 0.6$  m and  $T = 2.67$  sec).

Equations (1) and (2) are applied to evaluate these velocities at the sand surface according to the small-amplitude theory [2][3]. An empirical equation (Eq. (3)), proposed by Hanson and Cameron [4], is then used to determine the threshold velocities  $U_{w,cr}$  (m/s) for the motion inception of non-cohesive sediment under turbulent wave conditions.

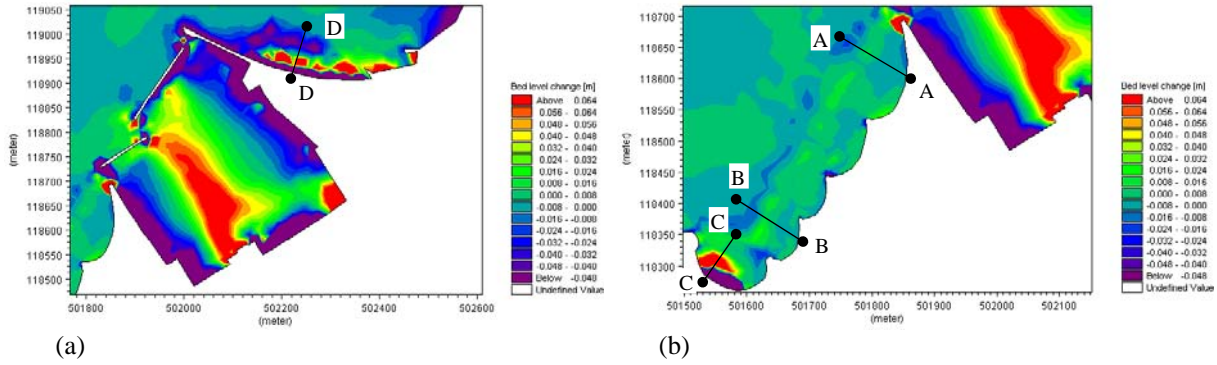


**Figure 5:** Bed erosion and deposition after an equivalent prototype simulation of 12 days for a “Bise” of  $T_W=5$  years. a) View of the north beach and the harbor, b) View of the south beach.

$$U_{\max} = \frac{\pi \cdot H}{T \cdot \sinh(2\pi \cdot d/L)}, \quad (1)$$

where,  $H$  is the wave height (m),  $T$  the wave period (sec),  $L$  the wave length (m) obtained from Eq. (2) and  $d$  the water depth measured from the still water level to the sand surface (m).

$$L = \frac{g \cdot T^2}{2\pi} \tanh(2\pi \cdot d/L), \quad (2)$$

The threshold velocities  $U_{w,cr}$  is given by:

$$U_{w,cr} = 0.5 \cdot \sqrt{((s-1) \cdot g)^{1.25} \cdot d_{50,cr}^{0.75} \cdot T^{0.5}}, \quad (3)$$

where,  $s = \rho_s/\rho$  is the relative density of the sediment in which  $\rho_s$  and  $\rho$  are the sediment and water densities ( $\text{kg/m}^3$ ). Table 3 resumes the estimated values of  $d_{50,cr}$  for the projected beaches.

Return period, $T_W$ (year)	Critical median diameters of beaches' sands, $d_{50,cr}$ (mm)			
	South beach (A-A)	South beach (B-B)	South beach (C-C)	North beach (D-D)
1	8.3	6.5	11.5	11.6
20	6.1	8.9	14.5	17.6
100	6.8	8.1	14.8	20.2

**Table 3:** Critical median diameters  $d_{50,cr}$  of beaches' sands for “Bise” with  $T_W = 1, 20$  and 100 years.

Figure 5.a shows a sediment deposition of about 6.4 cm in the middle of the harbor and an erosion of 4.8 mm at the toe of the harbor's walls. Table 3 shows that the backfill sands should have a median grain size diameter above 20 mm for the north beach, 15 mm around Section C-C and 9 mm all along the remaining part of the south beach.

### 3. PHYSICAL MODELING

#### 3.1 Objectives

The objective of the physical model is to validate the numerical results concerning notably the wave heights inside the port and the sediment transportation processes all along the beaches under the “Bise” load condition. It also aims to test different design proposals regarding the type of the protection dikes (rockfill and concrete barriers on piers) and the number and orientation of groins needed to protect the south beach.

#### 3.1 Physical set-up

A geometric distorted model was built with distorted horizontal and vertical scales of 1/150 and 1/75 respectively (Figure 6.a). The distortion factor of 2 is considered as acceptable for such type of modelisation [5]. The validity of such physical modeling of long waves (tidal models) stems from the fact that long waves have small vertical acceleration of water particles. The physical model covers the same area as the small numerical one. Working in a shallow wave reservoir, the wavelength is much greater than the depth and the distorted scaling criteria  $N_L (= L_p/L_m)$  is given by the expression:

$$N_L = N_T \cdot \sqrt{N_g \cdot N_h} , \quad (4)$$

where  $L_p$  and  $L_m$  are the wave lengths in prototype and model respectively,  $N_T$  the wave period ratio,  $N_g$  the gravitational ratio ( $=1$ ) and  $N_h$  the wave height ratio.

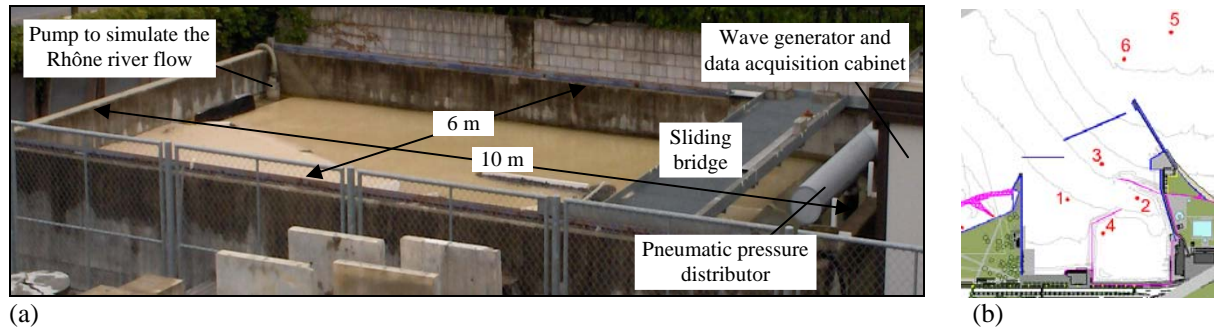


**Figure 6:** Physical model set-up. a) Global view of the wave tank, b) A plan view showing the four ultrasound sensors used to measure the wave heights inside and outside the future harbor.

The grain size of the sediment used in the physical model was determined using the “Best Model” proposed by Kamphuis [3] in which the critical grain size diameter ratio  $N_d (= d_{cr,p}/d_{cr,m})$  can be expressed as:

$$N_d = N_h^{0.75} \cdot N_{K_s}^{0.25} , \quad (5)$$

where  $N_{K_s}$  is the ratio ( $K_{s_p}/K_{s_m}$ ) of the Strickler coefficients of the bed in the prototype and in the model respectively. For  $N_{K_s} = 75$  and  $d_{cr,p} = d_{50,cr,p} = 20$  mm (maximum median diameter in Table 3), the critical diameter in the physical model is equal to 0.27 mm. A Quartz sand of a grain size distribution between 0.1 and 0.3 mm was thus used as backfill sand for the entire physical model.

#### 3.2 Results and discussion

##### 3.2.1 Water waves

The monochromatic waves generated in the physical model are nearly sinusoidal with constant height, period and direction. Inside the harbor, the wave characteristics have a statistical variability with an irregular surface record. The spectral analysis approach [6] was used to evaluate the significant wave height in the harbor. The zero-order spectral momentum  $m_0$ , is obtained from the wave spectrum  $E(f)$  ( $f$  being the frequency) of the discrete time series of the measured water surface. By assuming a Rayleigh distributed wave heights,  $H_s$  can be approximated by:

$$H_s = 3.8 \cdot \sqrt{m_0} , \quad (6)$$

Two different configurations for the west dikes were tested representing respectively rockfill dams and concrete barriers mounted on two parallel series of cylindrical piers. Also, two different lengths for the north protection dike (160 and 185 m) were examined. A syntthetic foam was used to model the absorbent version of the harbore’s walls. Results are presented in Table 4 for a “Bise” of  $T_W = 20$  years. The same general behavior was observed for the return periods of 1 and 100 years.

The experimental results from the two configurations were used for comparison with the numerical calculations. The numerical and physical wave heights of Case 1 (Figure 7.a) shows a good agreement with a maximum relative difference of 32%. The physical results in Case 2 are however far from those obtained numerically (Figure 7.b). This can be explained by the fact that the foam used to model the absorbent walls on the physical model did not have the same reflective coefficient as the one introduced in the numerical model. Nevertheless, the attenuation of the wave height inside the harbor can be confirmed numerically and physically when absorbent walls are adopted.

Geometrical configuration				Significant wave height on prototype scale, $H_s$ (m)				
Case	West dikes	North dike length (m)	Interior walls	Sensor 1	Sensor 3	Sensor 7	Sensor 8	Mean of all sensors
1	Rockfill	160	Reflective	0.311	0.189	0.253	0.173	0.232
2	Rockfill	160	Absorbent	0.214	0.103	0.162	0.110	0.147
3	Concrete barriers on piers	160	Reflective	0.512	0.400	0.397	0.249	0.390
4	Concrete barriers on piers	160	Absorbent	0.499	0.217	0.359	0.223	0.325
5	Concrete barriers on piers	185	Reflective	0.316	0.440	0.307	0.438	0.375
6	Concrete barriers on piers	185	Absorbent	0.359	0.364	0.260	0.330	0.328

**Table 4:** Significant wave heights inside the harbor determined by spectral analysis of the physical data.

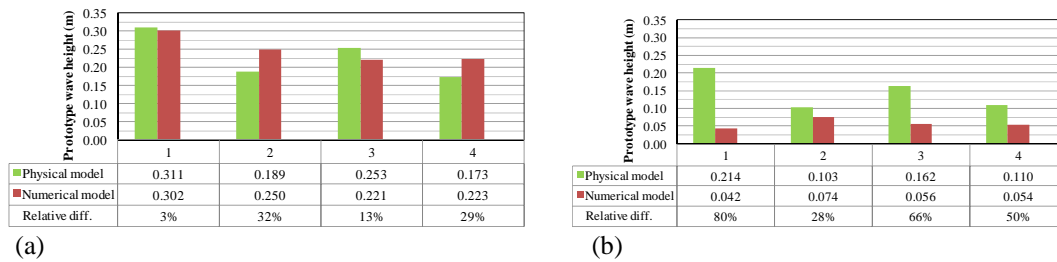


**Figure 7:** Comparison between prototype wave heights evaluated on both numerical and physical models. a) Results for Case 1 with Rockfill west dikes, short north dike and reflective walls, b) Results for Case 2 with Rockfill west dikes, short north dike and absorbent walls.

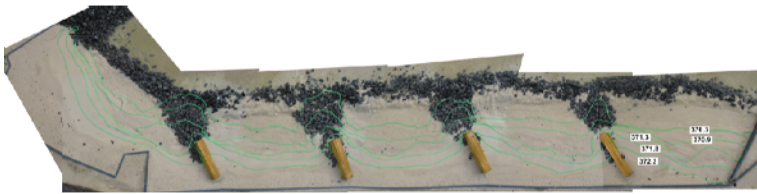
### 3.2.2 Sediment transport

Figure 8 shows five different south beach configurations tested. The duration of each test was equal to 3 hours with a load excitation corresponding to a return period  $T_W = 20$  years. An angle of 30 degrees north or south, relative to the coastline normal direction, was chosen in the configurations with inclined groins series. The erosion and deposition intensities were evaluated at the end of each test by visual observations (photos) and by surveying five bathymetric lines all along the beach. Results helped to select the most interesting configuration (Figure 9) to preserve the beach from excessive erosion and to maintain a general coherent beach’s shape without steep slopes.

Concerning the north beach, physical tests showed an important erosion at the toe of the foreshore and a deposition at the backshore side. A long shore sediment transport toward the lake following the north dike direction was also detected. A progressive south-north submerged rockfill barrier was suggested to stop the above sand seepage.



**Figure 8:** Five different groins configurations tested to protect the south beach of the project.



**Figure 9:** The configuration selected for the south beach with 4 groins oriented 30 degrees South.

## 4. CONCLUSIONS

The meteorological analysis reveals the “Bise” as the most critical wind condition for the project. The numerical model results show that the water current created by the Rhône river outflow and the “Bise” effect generates high velocities of about 35 cm/s near the south beach foreshore. A series of groins was added and tested in a physical model. The configuration with 4 groins oriented 30° south were adopted. For water renewal duration, the numerical results show a low current velocity inside the future harbor. Therefore, an open channel going through the north dike was proposed to connect open and close waters. The water renewal duration near the beaches was estimated around 6 to 8 hours. The numerical model was also used to determine the height of waves that penetrate inside the harbor. The maximum wave height reaches 13 cm in both cases with reflective and absorbent walls. The difference is that in the former case the maximum heights are spreaded over the entire area of the harbor whereas in the latter case they are concentrated at the north-west side of it. In comparison to the actual situation of the harbor, the use of absorbent walls and dikes leads to relative attenuation of the mean wave height of around 33%. Physical tests were conducted to study the influence of the protection dikes and harbor’s walls configurations on the transmission of waves inside the harbor. The validation of the numerical calculations was done by comparing the results obtained physically from one common harbor configuration. An acceptable agreement between numerical and physical results was found with a mean relative difference of 19%. The results of the physical model show that the most efficient configuration of the harbor is in which rockfill west dikes and absorbent walls are used. In this case, the mean wave heights expected inside the future harbor are around 15 cm.

Testing different project configurations using numerical modeling was time consuming. Such modeling was also ineffective for dikes made of concrete barrier on cylindrical piers. The physical modeling was a powerful tool to test the impact of beaches and harbor structures on wave heights and sediment transport. Nevertheless, the wave tank reveals some weaknesses regarding the influence of the boundary walls on the wave field. Due to the tank resonance phenomenon, it was difficult to generate waves with adequate periods and wave lengths. The complicity of both physical and numerical modeling has led to overcome the uncertainties and problems related to each modeling type and to converge toward an optimal project scheme.

## REFERENCES

- [1] Kamphuis, J. W. (2000). *Introduction to Coastal Engineering and Management*. Advanced Series on Ocean Engineering, Volume 16, World Scientific.
- [2] U.S. Army, Coastal Engineering Research Center (1973). *Shore Protection Manual*. Volume I, Second Edition. [www.archive.org/details/shoreprotectionm01coas](http://www.archive.org/details/shoreprotectionm01coas).
- [3] Bonnefille, R. (1992). *Cours d’hydraulique maritime*. Masson, 3<sup>rd</sup> edition.
- [4] Hanson, H., & Camenen, B. (2007). Closed form solution for threshold velocity for initiation of sediment motion under waves. *Coastal Sediments Conf., New Orleans, Louisiana, USA*, 15-28.
- [5] Hughes, S.A. (1993). *Physical Models and Laboratory Techniques in Coastal Engineering*. Advanced Series on Ocean Engineering, Volume 7, World Scientific.
- [6] U.S. Army, Coastal Engineering Manual (2008). *Chapter 1, Water wave mechanics*. Volume I, Second Edition. EM 1110-2-1100, Part II. <http://140.194.76.129/publications/eng-manuals/>.
- [7] Boillat J.-L., Sayah S., Schleiss A. (2006). Approche méthodologique pour l’établissement d’un projet de protection de rives lacustres. *Wasser Energie Luft*, Heft n° 4, December, 304-312.